

# Single top squark production as a probe of natural supersymmetry at the LHC

Ken-ichi Hikasa,<sup>1,\*</sup> Jinmian Li,<sup>2,†</sup> Lei Wu,<sup>3,‡</sup> and Jin Min Yang<sup>4,1,§</sup>

<sup>1</sup>*Department of Physics, Tohoku University, Sendai 980-8578, Japan*

<sup>2</sup>*ARC Centre of Excellence for Particle Physics at the Terascale, Department of Physics,  
University of Adelaide, Adelaide, South Australia 5005, Australia*

<sup>3</sup>*ARC Centre of Excellence for Particle Physics at the Terascale, School of Physics,  
The University of Sydney, Sydney, New South Wales 2006, Australia*

<sup>4</sup>*Institute of Theoretical Physics, Academia Sinica, Beijing 100190, People's Republic of China*  
(Received 1 June 2015; revised manuscript received 25 September 2015; published 4 February 2016)

Light top squarks (stops) and light higgsinos are the key features of natural supersymmetry (SUSY), where the higgsinos  $\tilde{\chi}_1^\pm$  and  $\tilde{\chi}_{1,2}^0$  are nearly degenerate and act as the missing transverse energy ( $E_T$ ) at the LHC. Besides the pair production via strong interaction, the stop can be produced via the electroweak interaction. The determination of the electroweak properties of the stop is an essential task for the LHC and future colliders. So, in this paper, we investigate the single stop ( $\tilde{t}_1$ ) production  $pp \rightarrow \tilde{t}_1 + E_T$  via the electroweak interaction in natural SUSY at the LHC, which gives the monotop signature  $t + E_T$  from  $\tilde{t}_1 \rightarrow t\tilde{\chi}_{1,2}^0$  or the monobottom signature  $b + E_T$  from  $\tilde{t}_1 \rightarrow b\tilde{\chi}_1^+$ . We perform Monte Carlo simulations for these signatures and obtain the observations: (1) The signal  $b + E_T$  has a better sensitivity than  $t + E_T$  for probing natural SUSY; (2) the parameter region with a higgsino mass  $100 \text{ GeV} \lesssim \mu \lesssim 225 \text{ GeV}$  and stop mass  $m_{\tilde{t}_1} \lesssim 620 \text{ GeV}$  can be probed through such single stop production with  $S/\sqrt{B} > 3$  and  $4\% \lesssim S/B \lesssim 19\%$  at the 14 TeV LHC with an integrated luminosity of  $3000 \text{ fb}^{-1}$ .

DOI: 10.1103/PhysRevD.93.035003

## I. INTRODUCTION

The search for supersymmetry (SUSY) is a long-standing important task in particle physics. One prime motivation for weak-scale SUSY is that it protects the Higgs vacuum expectation value without unnatural fine-tuning of the theory parameters. In the minimal supersymmetric standard model (MSSM), only a small subset of the supersymmetric partners strongly relates with the naturalness of the Higgs potential [1]. This can be seen from the minimization of the Higgs potential [2]:

$$\begin{aligned} \frac{M_Z^2}{2} &= \frac{(m_{H_d}^2 + \Sigma_d) - (m_{H_u}^2 + \Sigma_u)\tan^2\beta}{\tan^2\beta - 1} - \mu^2 \\ &\approx -\mu^2 - (m_{H_u}^2 + \Sigma_u), \end{aligned} \quad (1)$$

where  $\mu$  is the higgsino mass parameter, and  $m_{H_d}^2$  and  $m_{H_u}^2$  denote the weak-scale soft SUSY breaking masses of the Higgs fields. A moderate or large  $\tan\beta \equiv v_u/v_d$  is assumed in the last approximate equality.  $\Sigma_u$  and  $\Sigma_d$  arise from the radiative corrections to the Higgs potential, and the one-loop dominant contribution to  $\Sigma_u$  is given by [3]

$$\Sigma_u \sim \frac{3Y_t^2}{16\pi^2} \times m_{\tilde{t}_1}^2 \left( \log \frac{m_{\tilde{t}_1}^2}{Q^2} - 1 \right). \quad (2)$$

In order to obtain the observed value of  $M_Z$  without large cancellations in Eq. (1), each term on the right-hand side should be comparable in magnitude. Thus, the higgsino mass  $\mu$  must be of the order of  $\sim 100\text{--}200 \text{ GeV}$  and the requirement of  $\Sigma_u \sim M_Z^2/2$  produces an upper bound on the stop mass, which is about  $500 \text{ GeV}$  [4,5] (a  $125 \text{ GeV}$  Higgs mass can be achieved by a large stop trilinear coupling without very heavy stops in the MSSM or achieved by extending the MSSM with additional D terms or F terms [6–8]). In addition, since the gluino contributes to  $m_{H_u}$  at two-loop level, it is upper bounded by the naturalness [9] (however, the direct LHC searches have pushed the gluino up to TeV scale [10,11] while the recent ATLAS Z-peaked excess may indicate a gluino around  $800 \text{ GeV}$  [12]).

So, to test SUSY naturalness, the crucial task is to search for light stops or higgsinos. The search strategy for the pair productions of these nearly degenerate higgsinos has been recently studied [13–26]. During the LHC Run 1, the ATLAS and CMS collaborations have performed extensive searches for the stops through the gluino-mediated stop production [27,28] or the direct stop pair production [29,30]. Meanwhile, many theoretical studies that aim for improving the LHC sensitivity to a light stop have been proposed [31–46]. The current LHC constraints indicate a stop mass bound of hundreds of GeV [47–57].

---

\*hikasa@phys.tohoku.ac.jp  
†jinmian.li@adelaide.edu.au  
‡leiwu@physics.usyd.edu.au  
§jmyang@itp.ac.cn

However, these results are affected by the stop polarization states and branching ratios. The constraints on the right-handed stop from the LHC Run 1 direct searches [29,30] are usually weakened by the branching ratio suppression, which can still be as light as 230 GeV in some compressed region [58]. If the stop mass is heavier than about 450 GeV, it is allowed in most parameter space. So, in our work, we require the stop mass be heavier than 450 GeV [58].

Usually, the stop pair production provides the most sensitive way to search for the stop at the LHC. However, the stop can also participate in the electroweak interaction processes. The test of the electroweak properties of the stop is an essential task for the LHC and future colliders. In this work, we study the single stop production  $pp \rightarrow \tilde{t}_1 + E_T$  via the electroweak interaction in natural SUSY at the LHC. The observation of such single stop production will test the electroweak properties of the stop and the naturalness of supersymmetry.

This work is organized as follows. In Sec. II, we present our calculations and Monte Carlo simulations. In Sec. III, we show our results and give some discussions. Finally, in Sec. IV we draw our conclusions.

## II. CALCULATIONS AND SIMULATIONS

At the LHC, the single stop production is induced by the electroweak interaction and proceeds through the following process (see Fig. 1 for the corresponding Feynman diagrams):

$$pp \rightarrow \tilde{t}_1 \tilde{\chi}_1^- \quad (3)$$

Since in natural SUSY the light higgsinos are nearly degenerate, the decay products of  $\tilde{\chi}_1^- \rightarrow W^* \chi_1^0$  will carry

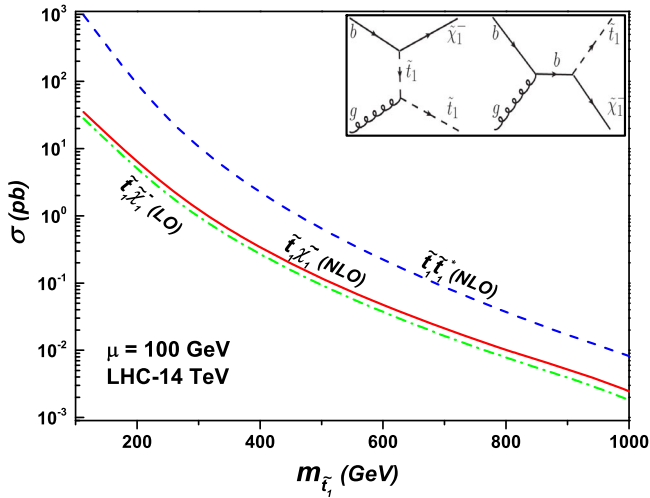


FIG. 1. The cross sections of  $\tilde{t}_1 \tilde{t}_1^*$  and  $\tilde{t}_1 \tilde{\chi}_1^-$  productions at the 14 TeV LHC for  $\tan\beta = 50$  and degenerate higgsinos with mass  $\mu = 100$  GeV. The contribution of conjugate process  $\tilde{t}_1^* \tilde{\chi}_1^+$  is included.

small energies and, hence, are too soft to be observed in the detector. Thus, the associated production of  $\tilde{t}_1 \tilde{\chi}_1^-$  can be identified as  $\tilde{t}_1 + E_T$ , which provides a distinctive signature at the LHC.

In Fig. 1, we show the next-to-leading-order (NLO) cross sections of the stop pair and the single stop productions for  $\mu = 100$  GeV at the 14 TeV LHC by using the packages Prospino2 [59] and MadGolem [60], respectively. The renormalization and factorization scales are taken as the average of the final states' masses. In the calculations of  $\tilde{t}_1 \tilde{\chi}_1^-$ , we use the LO and NLO parton densities given by CTEQ6L1 and CTEQ6M with five active flavors [61]. The contribution of the conjugate process  $\tilde{t}_1^* \tilde{\chi}_1^+$  is included. Except for the higgsino mass parameter  $\mu$  and right-handed stop soft mass  $m_{U_3}$ , we assume other soft supersymmetric masses at 1 TeV, and use the packages SOFTSUSY-3.3.9 [62] and MSSMcalc [63] to calculate masses, couplings and branching ratios of the sparticles. Since the cross section of single stop production is not sensitive to  $\tan\beta$ , we take  $\tan\beta = 50$  for simplicity. We find that the single stop cross section can still reach about 200 fb when  $m_{\tilde{t}_1} \simeq 450$  GeV. The NLO  $K$  factor of the process  $pp \rightarrow \tilde{t}_1 \tilde{\chi}_1^-$  ranges from 1.25 to 1.33. When the stop becomes heavy, the single stop production cross section will decrease, but slower than the pair production, due to the kinematics.

Next, we investigate the LHC observability of the single stop signatures with the sequent decays  $\tilde{t}_1 \rightarrow t \tilde{\chi}_{1,2}^0$  and  $\tilde{t}_1 \rightarrow b \tilde{\chi}_1^\pm$ :

$$pp \rightarrow \tilde{t}_1 \tilde{\chi}_1^- \rightarrow t \tilde{\chi}_{1,2}^0 \tilde{\chi}_1^- \rightarrow b j j + E_T, \quad (4)$$

$$pp \rightarrow \tilde{t}_1 \tilde{\chi}_1^- \rightarrow b \tilde{\chi}_1^\pm \tilde{\chi}_1^\mp \rightarrow b + E_T. \quad (5)$$

For the decay  $\tilde{t}_1 \rightarrow t \tilde{\chi}_{1,2}^0$ , the SM backgrounds to the signal<sup>1</sup>  $b j j + E_T$  are from the semi- and full-hadronic  $t\bar{t}$  events [64–66], where the undetected lepton and the limited jet energy resolution will lead to the relatively large missing transverse energy. The processes  $W +$  jets and  $Z +$  jets can fake the signal when one of those light-flavor jets are mistagged as a  $b$  jet. Also, the single top can mimic our signal when the lepton from the  $W$  boson decay is missed at the detector. The  $t\bar{t} + V$  backgrounds are not considered in our simulations due to their small missing energy or cross sections compared to the above backgrounds.

In Fig. 2, we present the parton-level  $p_T$  distribution of the top quark in the channel  $\tilde{t}_1 \rightarrow t \tilde{\chi}_{1,2}^0$  for  $\mu = 100$  GeV at the 14 TeV LHC. It can be seen that, with the increase of stop mass, the top quark produced from stop decay is boosted and has larger  $p_T$ . So, in the analysis of the  $\tilde{t}_1 \rightarrow t \tilde{\chi}_{1,2}^0$  channel, we respectively adopt HEPToptagger

<sup>1</sup>In Ref. [64] the authors comparatively studied the leptonic and hadronic monotop signals and found that the sensitivities of both signals are very close.

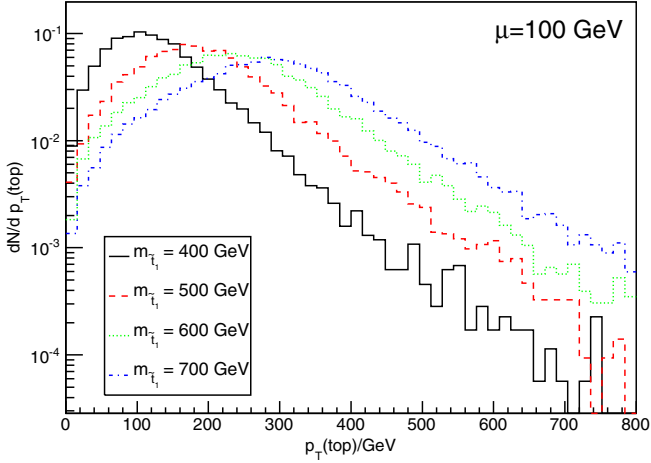


FIG. 2. The parton-level  $p_T$  distribution of the top quark in the channel  $\tilde{t}_1 \rightarrow \tilde{t}\tilde{\chi}_1^0$  for  $\mu = 100$  GeV at the 14 TeV LHC.

[32] and normal hadronic top reconstruction methods for each sample to identify the top quark in the final states and present our results with the best one. The detailed analysis strategies are the following:

- (i) Events with any isolated leptons are rejected.
- (ii) Method 1: We use Cambridge-Aachen algorithms [67] in Fastjet [68] to cluster the jets with  $R = 1.5$  to obtain the *top-jet* candidates. Each candidate must have the top quark substructure required by the HEPTopTagger. The *b* tagging is also imposed in the *top-jet* reconstruction. Other energy deposits outside the *top jet* are further reconstructed as the normal jets by using anti- $k_t$  algorithm with  $R = 0.4$  [69]. The top window used in our analysis is  $150 < m_t < 200$  GeV. While the  $W$  window is taken as the default value in HEPTopTagger.
- (iii) Method 2: In normal hadronic top quark reconstruction, a pair of jets is selected with the invariant mass  $m_{jj} > 60$  GeV and the smallest  $\Delta R$ . A third jet closest to this dijet system is used to constitute the top quark candidate. Among these three jets, at least one *b* jet and  $\Delta\phi(E_T, p_T(b_1)) > 1$  are required. The anti- $k_t$  algorithm is used for jet clustering with  $R = 0.4$ .
- (iv) We keep the events with one reconstructed top quark  $150 \text{ GeV} < m_t^{\text{rec}} < 200 \text{ GeV}$ .
- (v) The extra leading jet  $j_1$  outside the reconstructed top quark object is vetoed if  $p_T(j_1) > 30$  GeV and  $|\eta(j_1)| < 2.5$ .
- (vi) We define the signal regions according to  $(E_T, p_T(j_{\text{top}}))$  cuts  $(200, 100), (250, 150), (300, 200), (350, 250)$  for method 1, and  $(p_T(b), E_T)$  cuts  $(200, 50), (250, 50), (300, 100), (350, 100)$  GeV for method 2.

For the decay  $\tilde{t}_1 \rightarrow b\tilde{\chi}_1^+$ , the SM backgrounds to the signal  $b + E_T$  are dominated by the processes  $W + \text{jets}$  and

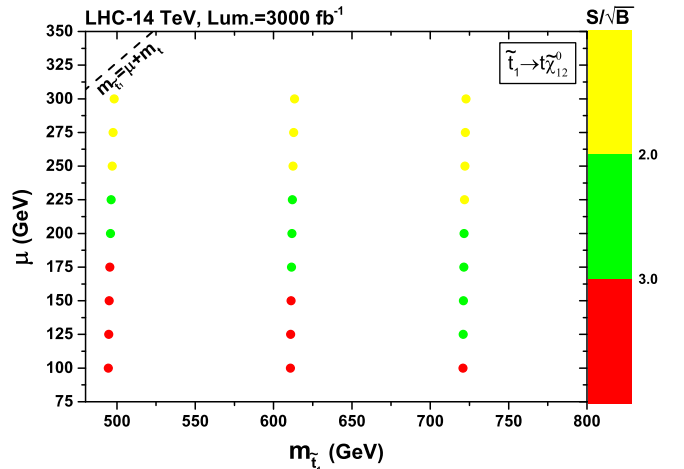


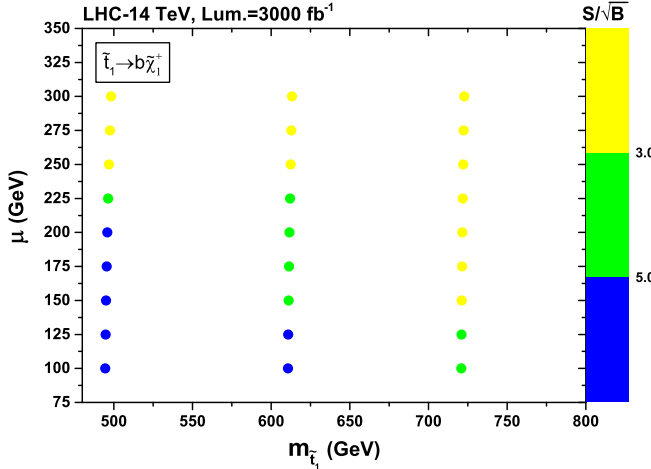
FIG. 3. The dependence of the significance of the channel  $\tilde{t}_1 \rightarrow \tilde{t}\tilde{\chi}_1^0$  on the higgsino mass  $\mu$  and stop mass  $m_{\tilde{t}_1}$  at the 14 TeV LHC with  $\mathcal{L} = 3000 \text{ fb}^{-1}$ .

$Z + \text{jets}$  when the light-flavor jets are misidentified as *b* jets [70]. The  $t\bar{t}$  events become the subleading backgrounds due to their large multiplicity. The signal events are selected to satisfy the following criteria:

- (i) Events with any isolated leptons are rejected.
- (ii) We require one hard *b* jet in the final states, but allow an additional softer jet with  $p_T(j_1) < 30$  GeV and  $\Delta\phi(E_T, p_T(j_1)) > 2$ . Since the hardness of the *b* jet from stop decay depends on the mass splitting between  $\tilde{t}_1$  and  $\tilde{\chi}_1^-$ , we define three signal regions for each sample according to  $(E_T, p_T(b))$  cuts:  $(100, 70), (150, 100)$  and  $(250, 200)$  GeV.

Finally, we use the most sensitive signal region (with the highest  $S/\sqrt{B}$ ) for each decay mode and show our results in Figs. 3 and 4, respectively. In our study, we omitted the QCD multijet backgrounds, whose correct treatment needs the experimental data-driven methods and hence depends on the realistic detector environments of the 14 TeV LHC. As discussed in [64,70,71], the requirements of high  $p_T(b_1)$  and large  $E_T$  with a separation  $\Delta\phi(E_T, p_T(j_1))$  can usually be expected to greatly reduce the fake contamination from the QCD backgrounds and allow for a good signal selection efficiency.

The parton-level signal and background events are generated with MadGraph5 [72], where  $W/Z + \text{jets}$  is matched up to three jets by using the matching scheme proposed in [73] and setting  $xqcut = 30$  GeV. For the value of  $qcut$  in matching, we take it to  $\max(xqcut + 5, xqcut * 1.2)$  [74] in our simulation. We perform parton shower and fast detector simulations with PYTHIA [75] and Delphes [76]. We assume the *b*-jet tagging efficiency as 70% [77] and a misidentification efficiency of *c* jets and light jets as 10% and 0.1%, respectively. The cross section of  $t\bar{t}$  is normalized to the approximately next-to-next-to-leading-order value  $\sigma_{t\bar{t}} = 920 \text{ pb}$  [78].

FIG. 4. Same as Fig. 3, but for the decay channel  $\tilde{t}_1 \rightarrow b\tilde{\chi}_1^+$ .

### III. RESULTS AND DISCUSSIONS

In Table I, we compare the results of  $pp \rightarrow \tilde{t}_1(\rightarrow \tilde{t}\tilde{\chi}_{1,2}^0)\tilde{\chi}_1^-$  for a benchmark point  $(m_{\tilde{t}_1}, \mu) = (611, 100)$  GeV in method 1 and method 2 at the 14 TeV LHC. From this table we can see that the  $Z + \text{jets}$  background in method 1 is smaller than in method 2, while the  $t\bar{t}$  background in method 1 is larger than in method 2. However, the signal events can be more kept in method 1 than in method 2. So the overall effects make method 1 have a better sensitivity in reconstructing the top quark in the region with a large mass splitting between  $\tilde{t}_1$  and  $\tilde{\chi}_1^-$ . At the 14 TeV LHC with  $\mathcal{L} = 3000 \text{ fb}^{-1}$ , the statistical significance  $S/\sqrt{B}$  for our benchmark point can reach  $3.9\sigma$  ( $2.1\sigma$ ) with  $S/B = 4.0\%$  ( $3.2\%$ ) in method 1 (2).

In Table II, we show the cross sections of  $V + \text{jets}$ ,  $t\bar{t}$  and  $\tilde{t}_1(\rightarrow b\tilde{\chi}_1^+)\tilde{\chi}_1^-$  for a benchmark point  $(m_{\tilde{t}_1}, \mu) = (496, 200)$  GeV at the 14 TeV LHC. Different from the  $\tilde{t}_1 \rightarrow \tilde{t}\tilde{\chi}_{1,2}^0$  channel, the  $Z + \text{jets}$  background is dominant over  $t\bar{t}$  since only one hard  $b$  jet is required in the final state. From Table II we can see that  $S/\sqrt{B}$  and  $S/B$  can reach 5.5% and 5.1% for  $\mathcal{L} = 3000 \text{ fb}^{-1}$ , respectively.

In Fig. 3, we display the dependence of statistical significance  $S/\sqrt{B}$  of the channel  $\tilde{t}_1 \rightarrow \tilde{t}\tilde{\chi}_{1,2}^0$  on the higgsino mass  $\mu$  and stop mass  $m_{\tilde{t}_1}$  at the 14 TeV LHC with  $\mathcal{L} = 3000 \text{ fb}^{-1}$ . We can see that values of  $S/\sqrt{B}$  decrease with the increase of  $\mu$  because of the cut

TABLE I. The cross sections of  $V + \text{jets}$ ,  $t\bar{t}$  and  $\tilde{t}_1(\rightarrow \tilde{t}\tilde{\chi}_{1,2}^0)\tilde{\chi}_1^-$  for a benchmark point  $(m_{\tilde{t}_1}, \mu) = (611, 100)$  GeV and  $\tan\beta = 10$  in method 1 and method 2 at the 14 TeV LHC with  $\mathcal{L} = 3000 \text{ fb}^{-1}$ . The cross sections are in unit of fb.

Cuts	$W + \text{jets}$	$Z + \text{jets}$	$t\bar{t}$	$tW$	$S$	$S/B$	$S/\sqrt{B}$
Method 1	$< 10^{-2}$	0.29	2.20	0.80	0.13	4.0%	3.9
Method 2	$< 10^{-2}$	0.59	0.55	0.24	0.044	3.2%	2.1

TABLE II. The cross sections of  $V + \text{jets}$ ,  $t\bar{t}$  and  $\tilde{t}_1(\rightarrow b\tilde{\chi}_1^+)\tilde{\chi}_1^-$  for a benchmark point  $(m_{\tilde{t}_1}, \mu) = (496, 200)$  GeV and  $\tan\beta = 10$  at the 14 TeV LHC with  $\mathcal{L} = 3000 \text{ fb}^{-1}$ . The cross sections are in unit of fb.

$W + \text{jets}$	$Z + \text{jets}$	$t\bar{t}$	$S$	$S/B$	$S/\sqrt{B}$
$< 10^{-2}$	2.77	1.10	0.20	5.1%	5.5

efficiency reduction. When the stop becomes heavy, the cross section of  $\tilde{t}_1\tilde{\chi}_1^-$  is suppressed. However, as a result of the application of the HEPTOPtagger method, more signal events can be kept, in particular in the mass range  $450 \text{ GeV} \lesssim m_{\tilde{t}_1} \lesssim 650 \text{ GeV}$ . Therefore, when  $\mu \lesssim 150 \text{ GeV}$ , the stop mass  $m_{\tilde{t}_1} \lesssim 610 \text{ GeV}$  can be probed at  $\gtrsim 3\sigma$  statistical significance with  $S/B \lesssim 8\%$ .

In Fig. 4, the statistical significance  $S/\sqrt{B}$  of the channel  $\tilde{t}_1 \rightarrow b\tilde{\chi}_1^+$  is presented on the plane of higgsino mass  $\mu$  versus stop mass  $m_{\tilde{t}_1}$  at the 14 TeV LHC with  $\mathcal{L} = 3000 \text{ fb}^{-1}$ . It can be seen that the sensitive stop region lies in  $450 \text{ GeV} \lesssim m_{\tilde{t}_1} \lesssim 620 \text{ GeV}$ , where a hard  $b$  jet ( $p_T > 200 \text{ GeV}$ ) and the sizable  $E_T$  ( $E_T > 250 \text{ GeV}$ ) can be used to effectively suppress the backgrounds. But when the stop mass increases,  $S/\sqrt{B}$  will rapidly decrease. We see that the higgsino mass  $100 \text{ GeV} \lesssim \mu \lesssim 225 \text{ GeV}$  and the stop mass  $m_{\tilde{t}_1} \lesssim 620 \text{ GeV}$  can be covered at  $\gtrsim 3\sigma$  statistical significance with  $S/B$  varying from 4% to 19%.

### IV. CONCLUSIONS

At the LHC the stop pair production is via the strong interaction while the single stop production is via the electroweak interaction. The study of single stop production can test the electroweak properties of the stop, which is an essential task for the LHC and future colliders. In this work we studied the single stop production  $pp \rightarrow \tilde{t}_1 + E_T$  as a test of natural SUSY at the LHC (here the missing energy is from the nearly degenerate higgsinos). By analyzing the decay channels of the stop  $\tilde{t}_1 \rightarrow \tilde{t}\tilde{\chi}_{1,2}^0$  and  $\tilde{t}_1 \rightarrow b\tilde{\chi}_1^+$ , we obtained the obervations: (1) The decay  $\tilde{t}_1 \rightarrow b\tilde{\chi}_1^+$  has a better sensitivity than  $\tilde{t}_1 \rightarrow \tilde{t}\tilde{\chi}_{1,2}^0$ ; (2) the parameter region with a higgsino mass  $100 \text{ GeV} \lesssim \mu \lesssim 225 \text{ GeV}$  and a stop mass  $m_{\tilde{t}_1} \lesssim 620 \text{ GeV}$  can be covered with  $S/\sqrt{B} > 3$  and  $4\% \lesssim S/B \lesssim 19\%$  at the 14 TeV HL-LHC with an integrated luminosity of  $3000 \text{ fb}^{-1}$ . So the searches for the single stop production will directly test the naturalness of supersymmetry and the electroweak properties of the stop.

### ACKNOWLEDGMENTS

L. W. thanks David Lopez-Val and Dorival Goncalves for providing us the Madgolem package. This work was partly supported by the Grant-in-Aid for Scientific

Research (Grant No. 24540246) from Ministry of Education, Culture, Sports, Science and Technology (MEXT) of Japan, by the Australian Research Council, by the CAS Center for Excellence in Particle Physics (CCEPP), by the National Natural Science Foundation of

China (NNSFC) under Grants No. 11305049, No. 11275057, No. 11375001, No. 11405047, No. 11275245, No. 10821504 and No. 11135003, and by Specialized Research Fund for the Doctoral Program of Higher Education under Grant No. 20134104120002.

- 
- [1] R. Barbieri and G. F. Giudice, *Nucl. Phys.* **B306**, 63 (1988).
- [2] R. Arnowitt and P. Nath, *Phys. Rev. D* **46**, 3981 (1992).
- [3] H. Baer, Vernon Barger, Peisi Huang, Dan Mickelson, Azar Mustafayev, and Xerxes Tata, *Phys. Rev. D* **87**, 115028 (2013).
- [4] S. F. King, M. Muhlleitner, and R. Nevzorov, *Nucl. Phys. B* **860**, 207 (2012).
- [5] Z. Kang, J. Li, and T. Li, *J. High Energy Phys.* 11 (2012) 024.
- [6] T. Han, P. Langacker, and B. McElrath, *Phys. Rev. D* **70**, 115006 (2004).
- [7] Y. Zhang, H. An, X. d. Ji, and R. N. Mohapatra, *Phys. Rev. D* **78**, 011302 (2008).
- [8] J. Cao, Z. Heng, J. M. Yang, Y. Zhang, and J. Zhu, *J. High Energy Phys.* 03 (2012) 086.
- [9] C. Brust, A. Katz, S. Lawrence, and R. Sundrum, *J. High Energy Phys.* 03 (2012) 103.
- [10] G. Aad *et al.* (ATLAS Collaboration), *J. High Energy Phys.* 10 (2013) 130; S. Chatrchyan *et al.* (CMS Collaboration), *J. High Energy Phys.* 06 (2014) 055.
- [11] T. Cheng, J. Li, T. Li, and Q. S. Yan, *Phys. Rev. D* **89**, 015015 (2014).
- [12] G. Aad *et al.* (ATLAS Collaboration), *Eur. Phys. J. C* **75**, 318 (2015); **75**, 463(E) (2015); G. Barenboim *et al.*, arXiv:1503.04184; U. Ellwanger, *Eur. Phys. J. C* **75**, 367 (2015); B. Allanach, A. Raklev, and A. Kvellestad, *Phys. Rev. D* **91**, 095016 (2015); A. Kobakhidze, N. Liu, L. Wu, and J. M. Yang, *Phys. Rev. D* **92**, 075008 (2015); J. Cao, L. Shang, J. M. Yang, and Y. Zhang, *J. High Energy Phys.* 06 (2015) 152.
- [13] G. F. Giudice and A. Pomarol, *Phys. Lett. B* **372**, 253 (1996).
- [14] K. L. Chan, U. Chattopadhyay, and P. Nath, *Phys. Rev. D* **58**, 096004 (1998).
- [15] S. P. Martin, *Phys. Rev. D* **89**, 035011 (2014).
- [16] H. Baer, V. Barger, P. Huang, A. Mustafayev, and X. Tata, *Phys. Rev. Lett.* **109**, 161802 (2012).
- [17] I. Gogoladze, F. Nasir, and Q. Shafi, *Int. J. Mod. Phys. A* **28**, 1350046 (2013).
- [18] S. Gori, S. Jung, and L. T. Wang, *J. High Energy Phys.* 10 (2013) 191.
- [19] H. Baer, V. Barger, P. Huang, D. Mickelson, A. Mustafayev, W. Sreethawong, and X. Tata, *Phys. Rev. Lett.* **110**, 151801 (2013).
- [20] C. Han, A. Kobakhidze, N. Liu, A. Saavedra, L. Wu, and J. M. Yang, *J. High Energy Phys.* 02 (2014) 049.
- [21] P. Schwaller and J. Zurita, *J. High Energy Phys.* 03 (2014) 060.
- [22] Z. Han, G. D. Kribs, A. Martin, and A. Menon, *Phys. Rev. D* **89**, 075007 (2014).
- [23] H. Baer, A. Mustafayev, and X. Tata, *Phys. Rev. D* **90**, 115007 (2014).
- [24] C. Han, D. Kim, S. Munir, and M. Park, *J. High Energy Phys.* 04 (2015) 132.
- [25] D. Barducci, A. Belyaev, A. K. M. Bharucha, W. Porod, and V. Sanz, *J. High Energy Phys.* 07 (2015) 066.
- [26] A. G. Delannoy *et al.*, *Phys. Rev. Lett.* **111**, 061801 (2013).
- [27] G. Aad *et al.* (ATLAS Collaboration), *J. High Energy Phys.* **10** (2014) 24.
- [28] S. Chatrchyan *et al.* (CMS Collaboration), *Phys. Lett. B* **725**, 243 (2013).
- [29] G. Aad *et al.* (ATLAS Collaboration), *Phys. Rev. D* **90**, 052008 (2014); *J. High Energy Phys.* 11 (2014) 118; *Eur. Phys. J. C* **74**, 3109 (2014); *J. High Energy Phys.* 09 (2014) 015; **06** (2014) 124; **10** (2013) 189.
- [30] S. Chatrchyan *et al.* (CMS Collaboration), *Phys. Rev. Lett.* **112**, 161802 (2014); *Phys. Lett. B* **736**, 371 (2014); **743**, 503 (2015); *Eur. Phys. J. C* **73**, 2677 (2013); *J. High Energy Phys.* **06** (2015) 116.
- [31] Y. Bai, H. C. Cheng, J. Gallicchio, and J. Gu, *J. High Energy Phys.* **07** (2012) 110; **08** (2013) 085.
- [32] D. E. Kaplan, K. Rehermann, and D. Stolarski, *J. High Energy Phys.* **07** (2012) 119.
- [33] T. Plehn, M. Spannowsky, and M. Takeuchi, *J. High Energy Phys.* **08** (2012) 091; *Phys. Rev. D* **85**, 034029 (2012); *J. High Energy Phys.* **05** (2011) 135; T. Plehn, M. Spannowsky, M. Takeuchi, and D. Zerwas, *J. High Energy Phys.* **10** (2010) 078.
- [34] J. Thaler and K. Van Tilburg, *J. High Energy Phys.* **02** (2012) 093.
- [35] Z. Han, A. Katz, D. Krohn, and M. Reece, *J. High Energy Phys.* **08** (2012) 083.
- [36] M. Drees, M. Hanussek, and J. S. Kim, *Phys. Rev. D* **86**, 035024 (2012).
- [37] D. S. M. Alves, M. R. Buckley, P. J. Fox, J. D. Lykken, and C.-T. Yu, *Phys. Rev. D* **87**, 035016 (2013).
- [38] X.-J. Bi, Q.-S. Yan, and P.-F. Yin, *Phys. Rev. D* **85**, 035005 (2012).
- [39] J. Cao, C. Han, L. Wu, J. M. Yang, and Y. Zhang, *J. High Energy Phys.* **11** (2012) 039.
- [40] M. L. Graesser and J. Shelton, *Phys. Rev. Lett.* **111**, 121802 (2013).
- [41] G. Ferretti, R. Franceschini, C. Petersson, and R. Torre, *Phys. Rev. Lett.* **114**, 201801 (2015).
- [42] M. Czakon, A. Mitov, M. Papucci, J. T. Ruderman, and A. Weiler, *Phys. Rev. Lett.* **113**, 201803 (2014).

- [43] B. Fuks, P. Richardson, and A. Wilcock, *Eur. Phys. J. C* **75**, 308 (2015).
- [44] B. Nachman and C. G. Lester, *Phys. Rev. D* **88**, 075013 (2013).
- [45] T. Eifert and B. Nachman, *Phys. Lett. B* **743**, 218 (2015).
- [46] A. Ismail, R. Schwienhorst, J. S. Virzi, and D. G. E. Walker, *Phys. Rev. D* **91**, 074002 (2015).
- [47] M. Papucci, J. T. Ruderman, and A. Weiler, *J. High Energy Phys.* **09** (2012) 035.
- [48] L. J. Hall, D. Pinner, and J. T. Ruderman, *J. High Energy Phys.* **04** (2012) 131.
- [49] O. Buchmueller and J. Marrouche, *Int. J. Mod. Phys. A* **29**, 1450032 (2014).
- [50] G. D. Kribs, A. Martin, and A. Menon, *Phys. Rev. D* **88**, 035025 (2013).
- [51] C. Han, K.-i. Hikasa, L. Wu, J. M. Yang, and Y. Zhang, *J. High Energy Phys.* **10** (2013) 216.
- [52] K. Kowalska and E. M. Sessolo, *Phys. Rev. D* **88**, 075001 (2013).
- [53] M. Cahill-Rowley, J. Hewett, A. Ismail, and T. Rizzo, *Phys. Rev. D* **90**, 095017 (2014).
- [54] K. J. de Vries *et al.*, *Eur. Phys. J. C* **75**, 422 (2015).
- [55] H. Abe, J. Kawamura, and Y. Omura, *J. High Energy Phys.* **08** (2015) 089.
- [56] B. Batell and S. Jung, *J. High Energy Phys.* **07** (2015) 061.
- [57] A. Katz, M. Reece, and A. Sajjad, *J. High Energy Phys.* **10** (2014) 102.
- [58] M. Drees and J. S. Kim, arXiv:1511.04461.
- [59] W. Beenakker, M. Krämer, T. Plehn, M. Spira, and P. M. Zerwas, *Nucl. Phys.* **B515**, 3 (1998).
- [60] D. Goncalves, D. Lopez-Val, K. Mawatari, and T. Plehn, *Phys. Rev. D* **90**, 075007 (2014); D. Lopez-Val *et al.*, *Proc. Sci.*, LL 2012 (2012) 048; D. Goncalves D. Gonçalves-Netto, D. López-Val, K. Mawatari, T. Plehn, and I. Wigmore, *Phys. Rev. D* **87**, 014002 (2013).
- [61] J. Pumplin, D. R. Stump, J. Huston, H.-L. Lai, P. Nadolsky, and W.-K. Tung, *J. High Energy Phys.* **07** (2002) 012.
- [62] B. C. Allanach, *Comput. Phys. Commun.* **143**, 305 (2002).
- [63] M. Muhlleitner, A. Djouadi, and Y. Mambrini, *Comput. Phys. Commun.* **168**, 46 (2005).
- [64] J. L. Agram, J. Andrea, M. Buttignol, E. Conte, and B. Fuks, *Phys. Rev. D* **89**, 014028 (2014).
- [65] J. Andrea, B. Fuks, and F. Maltoni, *Phys. Rev. D* **84**, 074025 (2011).
- [66] J. Wang, C. S. Li, D. Y. Shao, and H. Zhang, *Phys. Rev. D* **86**, 034008 (2012).
- [67] Y. L. Dokshitzer, G. D. Leder, S. Moretti, and B. R. Webber, *J. High Energy Phys.* **08** (1997) 001.
- [68] M. Cacciari, G. P. Salam, and G. Soyez, *Eur. Phys. J. C* **72**, 1896 (2012).
- [69] M. Cacciari, G. P. Salam, and G. Soyez, *J. High Energy Phys.* **04** (2008) 063.
- [70] T. Lin, E. W. Kolb, and L. T. Wang, *Phys. Rev. D* **88**, 063510 (2013).
- [71] V. Khachatryan *et al.* (CMS Collaboration), *Phys. Rev. Lett.* **114**, 101801 (2015).
- [72] J. Alwall, M. Herquet, F. Maltoni, O. Mattelaer, and T. Stelzer, *J. High Energy Phys.* **06** (2011) 128.
- [73] F. Caravaglios, M. L. Mangano, M. Moretti, and R. Pittau, *Nucl. Phys.* **B539**, 215 (1999).
- [74] <https://cp3.irmp.ucl.ac.be/projects/madgraph/wiki/Matching>.
- [75] T. Sjostrand, S. Mrenna, and P. Z. Skands, *J. High Energy Phys.* **05** (2006) 026.
- [76] J. de Favereau, C. Delaere, P. Demin, A. Giannanco, V. Lemaître, A. Mertens, and M. Selvaggi, *J. High Energy Phys.* **02** (2014) 057.
- [77] CMS Collaboration, Report No. CMS-PAS-BTV-11-004, 2011.
- [78] N. Kidonakis, *Phys. Rev. D* **84**, 011504 (2011).